Materials and Design 59 (2014) 241–245

Contents lists available at ScienceDirect

Materials and Design

journal homepage: www.elsevier.com/locate/matdes

Metallic glass–steel composite with improved compressive plasticity

H. Shakur Shahabi [a,*], S. Scudino [a], U. Kühn [a], J. Eckert [a,b]

[a] IFW Dresden, Institut für Komplexe Materialien, Helmholtzstraße 20, D-01069 Dresden, Germany
[b] TU Dresden, Institut für Werkstoffwissenschaft, D-01062 Dresden, Germany

ARTICLE INFO

Article history:
Received 19 January 2014
Accepted 3 March 2014
Available online 12 March 2014

Keywords:
Composites
Metallic glasses
Brittleness and ductility
Mechanical properties at ambient temperature

ABSTRACT

A $Zr_{52.5}Cu_{18}Ni_{14.5}Al_{10}Ti_5$ bulk metallic glass toughened with a commercially available spring-shaped steel wire has been produced by centrifugal casting. The addition of the steel spring significantly affects shear band nucleation and propagation through the blockage, deflection and multiplication of shear bands at the glass–spring interface. As a result of the more homogeneous distribution of the plastic strain, the room temperature plasticity increases from 0.9% for the monolitic glass to about 4% for the glass–spring composite. Given the low volume fraction of the spring used in the composite (4.2 vol.%), these results demonstrate the extreme effectiveness of the steel spring for improving the plasticity of the metallic glass.

1. Introduction

Bulk metallic glasses (BMGs) have received much attention within the last decades due to their large elastic limit and high strength compared to their crystalline counterparts [1]. Despite these advantages, the limited room temperature plasticity of BMGs is still a major drawback which hinders the utilization of these materials in engineering applications. Plastic deformation of BMGs occurs through the formation of highly localized shear bands, which propagate quickly resulting in catastrophic failure soon after yielding [1].

A way to improve the plasticity of BMGs is the creation of bulk metallic glass composites (BMGCs), where the presence of a second phase in the amorphous matrix improves the plasticity via restricting shear bands propagation and through the generation of multiple shear bands [2–4]. BMGCs can be classified into two main categories according to the processing route used [5]: in situ and ex situ composites. In the ex situ composites, micro-/nano-sized particles, fibers or wires are added to the glassy matrix by using melt infiltration [6] or powder metallurgy [7,8], whereas in situ composites are produced directly during solidification through the appropriate choice of composition or cooling rate [5,9,10]. Alternatively, in situ composites can also be produced by controlled heat treatment of the monolithic glass to precipitate micro-/nano-sized crystalline phases from the amorphous matrix [5]. Although the in situ processing has the merit to simplify the process, the ex situ processing gives more freedom in tailoring the microstructure (e.g. size and volume fraction of the second phase).

Zr-based BMGs are of significant interest as glassy matrices in BMGCs thanks to their excellent glass forming ability and wide supercooled liquid region [2,11–14]. The second phases in these composites are fibers, whiskers or particles discontinuously distributed within the glassy matrix and their amount is rather large, generally exceeding 10 vol.%. Examples are the ex situ Zr-based BMGCs with second phases such as steel [2], W [2,14], Ta, Nb and Mo [12].

The homogeneous distribution of the second phases has a decisive effect on the mechanical properties of the resulting composites [15,16]. This is particularly critical for composites with discontinuously distributed second phases, where particles clustering may occur, consequently reducing their effectiveness as toughening or strengthening agents [17]. Recently, Wang et al. [18] have overcome this drawback through the creation of composites consisting of a BMG matrix and an open-cell Cu foam, which acts as a continuous three-dimensional deformable network. This approach is very effective for combating catastrophic shear banding of BMGs, given the extremely low volume fraction of the toughening second phase (4.2 vol.%): the room temperature plasticity increases from 2.5% for the monolithic BMG to 5.6% for the BMG composite [18].

In this work, we further examine this approach by using a steel spring as continuous second phase with reduced volume fraction to produce plastically deformable Zr-based BMGCs. The spring shape was selected in order to analyze the effect of a second phase with a well-defined geometry on the shear band evolution and resulting mechanical properties.

* Corresponding author. Tel.: +49 351 4659 878.
E-mail address: h.shakur.shahabi@ifw-dresden.de (H. Shakur Shahabi).

http://dx.doi.org/10.1016/j.matdes.2014.03.007
0261-3069/

2. Experimental details

BMG composites consisting of a glassy matrix with nominal composition $Zr_{52.5}Cu_{18}Ni_{14.5}Al_{10}Ti_5$ (at.%) and a commercially available spring-shaped steel wire were produced by centrifugal copper mold casting in the form of cylindrical samples with 4 mm diameter and 48 mm length. For this (see schematic illustration in Fig. 1(a)), the $Zr_{52.5}Cu_{18}Ni_{14.5}Al_{10}Ti_5$ alloy (produced by arc melting in a titanium-gettered argon atmosphere) was cast into the cylindrical copper die containing the steel spring (outer diameter ~2.8 mm, inter-ring spacing ~1.4 mm and wire thickness ~300 μm). For comparison, the monolithic $Zr_{52.5}Cu_{18}Ni_{14.5}Al_{10}Ti_5$ BMG was also produced using the same casting parameters (ejection temperature 1573 K; argon overpressure 100 mbar) as used for the glass–spring composite. Cylindrical specimens with aspect ratio of 2 (8 mm length and 4 mm diameter) were prepared from the cast rods and mechanically tested at room temperature using an Instron 8562 testing facility under quasistatic compressive loading (strain rate $\sim 1 \times 10^{-4}\,s^{-1}$). Both ends of the specimens were carefully polished to make them parallel to each other prior to the compression test. The compressive strain was measured directly on the specimens using a Fiedler laser-extensometer. To obtain the volume fraction of the steel spring in the composites, the density of the spring and BMGC were determined using the Archimedes principle, which gives a volume fraction of steel of 4.2%. The microstructure of the samples and their surface morphology after the mechanical tests were investigated by scanning electron microscopy (SEM) using a Gemini 1530 microscope coupled with energy-dispersive X-ray (EDX) analysis. The amorphous nature of the matrix in the specimens was verified by X-ray diffraction (XRD) using a Philips PW 1050 diffractometer (Co Kα radiation).

3. Results and discussion

Fig. 1(b) shows the SEM micrograph of the longitudinal cross section of the $Zr_{52.5}Cu_{18}Ni_{14.5}Al_{10}Ti_5$ BMG toughened with the steel spring. The spring (dark grey circles in Fig. 1(b)) is embedded in the glassy matrix (light grey area in Fig. 1(b)) and spirals continuously along the sample. Most of the glass–spring interfaces are continuous and free of porosity (Fig. 1(c)); however, imperfect interfaces and porosity (indicated by an arrow in Fig. 1(d)) can occasionally be observed. The good glass–spring interface can be ascribed to the low volume fraction and to the simple shape of the spring, through which the melt can flow easily and fill available gaps between the steel wires. In addition, the low surface roughness of the spring most likely prevents the turbulent flow of the melt at the interface, avoiding the formation of gaps, which may be quenched in the sample as a result of the fast cooling rate. Another important factor for affecting the glass–spring interface is the small difference of the coefficients of thermal expansion between steel and the $Zr_{52.5}Cu_{18}Ni_{14.5}Al_{10}Ti_5$ BMG ($4.06 \times 10^{-5}\,K^{-1}$ [19] and $3.9 \times 10^{-5}\,K^{-1}$ [20], respectively), which may prevent debonding at the interface during cooling.

EDX compositional analysis (Fig. 2(a)–(c)) for the two main elements Zr (red) and Fe (yellow) indicates that no visible interdiffusion of these elements between the glassy matrix and the steel spring occurs during sample preparation. The absence of interdiffusion is in contrast to the results reported by Wang et al. [18], who observed significant Cu diffusion from the Cu foam into the Ti-based BMG matrix. This contrasting behavior can be ascribed to the difference of cooling rate between centrifugal and suction casting [21] and to the resulting time spent by the alloy in the liquid state, where diffusion is faster. The absence of a reaction between glassy matrix and spring is confirmed by the XRD pattern of the composite (Fig. 2(d)): the pattern displays the broad diffuse maxima characteristic of the monolithic glass along with a sharp crystalline peak belonging to steel. No peaks due to any additional phases are detected.

The room temperature compressive stress–strain curves for the monolithic BMG and glass–spring composite are shown in Fig. 3(a). The monolithic glass exhibits an elastic regime of 1.9% before yielding, which occurs at about 1650 MPa. After yielding the stress slightly increases with increasing strain up to fracture, which takes place at 1700 MPa stress and 2.8% strain. This results in a plastic strain of 0.9%. The addition of the steel spring remarkably affects the mechanical properties of the material. Although the yield strength and the elastic limit (1450 MPa and 1.65%) are reduced

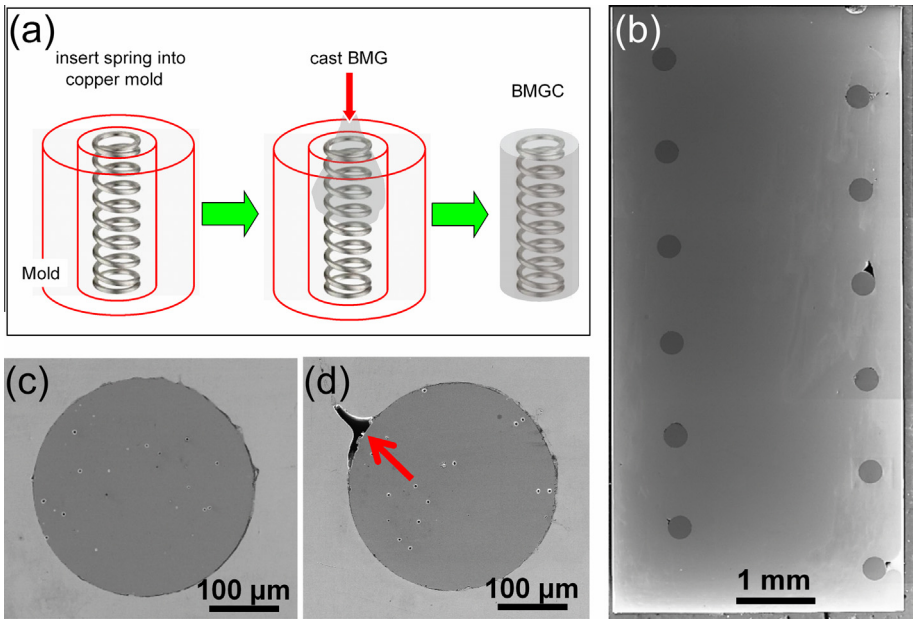

Fig. 1. (a) Schematic illustration of the preparation of the $Zr_{52.5}Cu_{18}Ni_{14.5}Al_{10}Ti_5$ glass–steel spring composite. SEM micrographs of (b) longitudinal cross-section of the glass–spring composite, (b) continuous, pore-free glass–spring interface and (c) interface with porosity (indicated by an arrow).

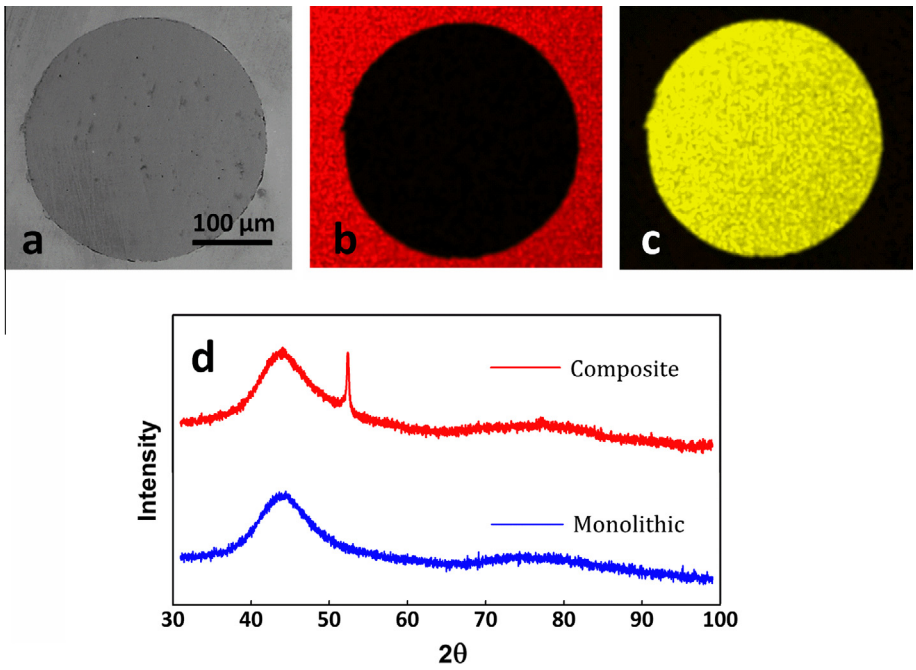

Fig. 2. (a) SEM micrograph and corresponding EDX compositional maps for (b) Zr (red) and (c) Fe (yellow). (d) XRD patterns for the monolithic BMG and glass–spring composite. (For interpretation of the references to color in this figure legend, the reader is referred to the web version of this article.)

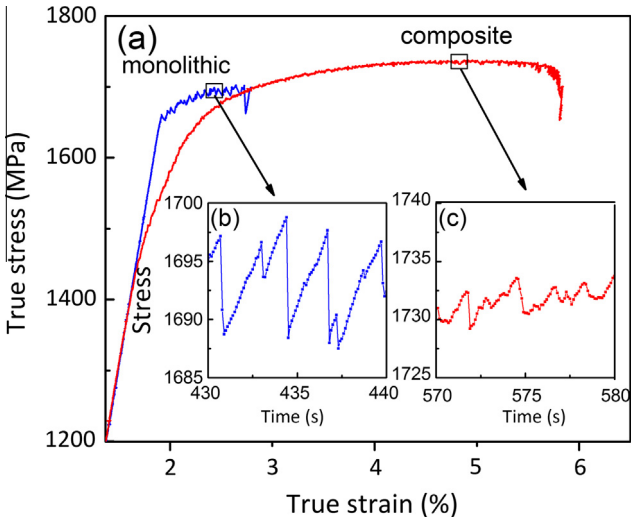

Fig. 3. (a) Room temperature compressive stress–strain curves for the monolithic BMG and glass–spring composite. Examples of the serration behavior during plastic deformation for the monolithic BMG (b) and BMG–spring composite (c).

compared to the monolithic glass, the composite displays a clear work-hardening behavior up to 1730 MPa where fracture occurs at 5.8% strain, which corresponds to a plastic deformation of about 4%. Young's modulus, calculated from the linear elastic range of the stress–strain curves, is 88 ± 3 GPa for the BMG and 86 ± 8 GPa for the BMGC. Therefore, the change of Young's modulus induced by addition of the steel spring predicted by the rule of mixture (91.5 GPa) is not observed, most likely because of the small volume fraction of the second phase and presence of residual porosity in the samples.

Fig. 4(a) and (b) shows the microstructural features, investigated by SEM, of the monolithic BMG and BMGC after compression tests. The outer surface of the monolithic glass (Fig. 4(a)) exhibits a limited number of shear bands, located exclusively near the fracture plane, which are oriented normal to the loading direction or parallel to the fracture surface. The composite displays a similar orientation of the shear bands but their number is much larger compared to the single-phase glass and their distribution covers the entire specimen (Fig. 4(b)). The fracture angle is about 42° for both the monolithic glass and BMGC, which conforms well to the reported values for the fracture angles of monolithic Zr-based BMGs under compressive loading [22]. This is in contrast to the fracture angle of 32°, which has been reported for particle reinforced or dendritic Zr-based BMG composites, where the normal stress significantly contributes to the fracture mode [22]. The smaller deviation of the fracture angle from 45° (the plane of maximum shear stress according to Tresca yield criterion) characterizing the present samples indicates that the fracture is less affected by the normal stress and that the shear stress plays a major role.

Plastically deformable ex situ and in situ Zr-based BMGCs has been produced by other researchers [11,23–27] using large fractions of discontinuously distributed small sized particles or fibers. Small-sized second phases result in large matrix-second phase interfaces; the resulting high interface mismatch stresses are responsible for the hindered shear bands propagation and, at the same time, they may induce the nucleation of additional shear bands [27,28]. This shear bands arrest/nucleation behavior can occur when the distance between the reinforcing particles is smaller than length-scale of the shear bands [22]. The current BMGC displays improved compressive plasticity despite having a large sized second phase (thickness ~300 μm), large distance between the wires (1.4 mm) and small volume fraction of the second phase (4.2 vol.%). This contradiction can be understood by considering the large difference of Young's modulus between steel and the Zr-based glassy matrix (210 and 84 GPa). This difference may create a considerable stress concentration at the glass–spring interface during elastic deformation, which then may trigger the nucleation of shear bands and initiate plastic deformation at much lower stresses compared to the monolithic glass, as observed in Fig. 3(a). The spring shape can also play a significant role in improving the plasticity through the creation of a uniform distribution of interface stress fields which cover all the angles from 0° to

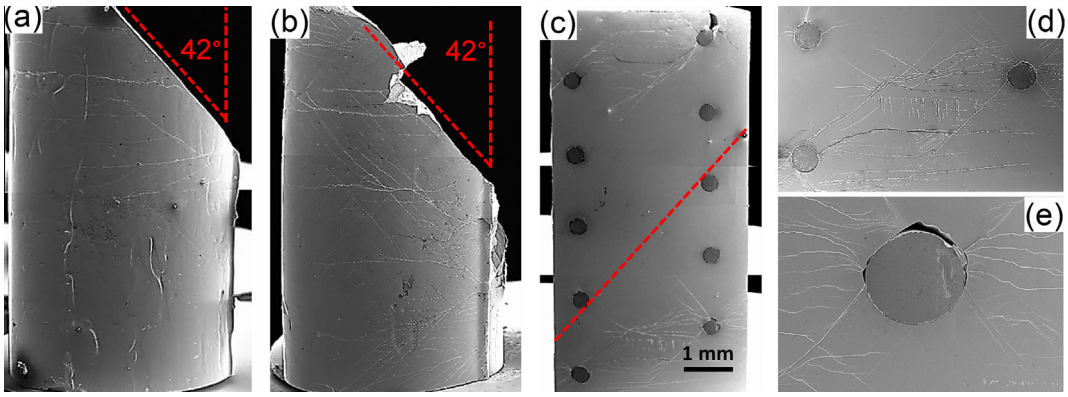

Fig. 4. SEM micrographs of the fracture morphology after compression tests for (a) monolithic BMG and (b) glass–spring composite. (c)–(e) Longitudinally-cut semi-circular composite specimen after compression test (stopped at a plastic strain of 1%), revealing significant shear band branching and deflection.

90° when the wire spirals through the height of the sample. This kind of arrangement may be very effective for hindering the propagation of shear bands followed by shear bands nucleation or branching.

The activation of a larger number of shear bands in the composite compared with the monolithic BMG can be tracked by a detailed investigation of the plastic region of the compressive stress–strain curves in Fig. 3(a). The observed flow serration behavior of metallic glasses during plastic deformation is known as an indication of shear band(s) arrest and propagation dynamics corresponding respectively to the load drop and rise in each serration [29–32]. Compared to the monolithic BMG (Fig. 3(b)), the glass–spring composite shows a flow serration characterized by a larger number of serrations per unit time with reduced amplitude (Fig. 3(c)). A similar behavior has been reported for Ti-based BMGCs toughened with Cu foam [18] and it resembles plastic deformation at high strain rates where the formation of multiple shear bands and their propagation is reflected by very fine or smoothed out serrations in the load–displacement curves [30]. Sun et al. [32] have shown that in such cases the deformation proceeds via the simultaneous operation of multiple shear bands, where each band contributes to the plasticity by carrying a very small amount of strain without causing catastrophic failure, finally leading to large room temperature plasticity. In such cases, shear bands inevitably interact with each other and thus affect their formation and propagation [32].

In order to analyze the effect of the glass–spring interface on the formation of shear bands, a compression test (stopped at a plastic strain of 1%) was performed on a longitudinally-cut semi-circular composite specimen and the morphology of the resulting shear bands was investigated by SEM (Fig. 4(c)–(e)). Although the shape of this sample does not provide an optimal stress distribution during testing, its flat surface nevertheless offers the opportunity to observe how the glass–spring interface affects shear banding. The formation of a high density of shear bands can be detected in the areas near the top and bottom of the sample (Fig. 4(c)). This may be ascribed to the frictional forces arising at the interface with the machine cross-heads, which create confining stresses resulting in multiple shear banding [33]. The shear bands nucleate at the glass–spring interfaces and their direction forms an angle of about 40–45° with respect to the loading direction (Fig. 4(d)). While propagating towards the center of the sample, some shear bands are branched or blocked by the glass–spring interfaces, whereas others are deflected towards the direction perpendicular to the loading direction (Fig. 4(e)), which clearly demonstrates that the steel spring represents an effective medium for inducing blockage, deflection and multiplication of shear bands in the glassy matrix.

The fracture of the sample with semicircular cross section (not shown here) occurs along a line connecting two opposite parts of the spring (see red[1] dashed line in Fig. 4(c)). The line makes an angle of about 42° with the loading direction, which is in excellent agreement with fracture angle observed for the conventional cylindrical specimens (~42°). The fracture of the composite is most likely governed by the crack formed through the connection of shear bands generated at the glass–spring interfaces, in agreement with recent findings [34–36] reporting that fracture is governed by cracks interconnecting heterostructures [34] or notches [35,36] created due to non-uniform stress distribution around artificially introduced artifacts. This explains the similarity of fracture angle between monolithic BMG and glass–spring composite and suggests that through the proper variation of the spring geometry (e.g. diameter and inter-ring spacing), the direction of the fracture plane may be manipulated to further enhance the deformability of the metallic glass.

4. Conclusions

In this work, the possibility to use a continuous second phase with reduced volume fraction and a well-defined geometry to produce ex situ Zr-based BMG composites with good room temperature plasticity was examined. To achieve this aim, a commercially available spring-shaped steel wire was used to toughen the $Zr_{52.5}Cu_{18}Ni_{14.5}Al_{10}Ti_5$ bulk metallic glass. The steel spring is very effective for improving the room temperature plastic deformability of the material, which increases from 0.9% for the monolitic glass to about 4% for the glass–spring composite. Microstructural investigations indicate that the glass–spring interface plays a major role through blockage, deflection and multiplication of shear bands. This can be ascribed to the large difference of Young's modulus between steel and the Zr-based glassy matrix that may create a considerable stress concentration at the glass–spring interface during elastic deformation, which then may induce shear bands branching and multiplication and, thus, a more homogeneous distribution of the plastic strain.

References

[1] Schuh CA, Hufnagel TC, Ramamurty U. Mechanical behavior of amorphous alloys. Acta Mater 2007;55:4067–109.
[2] Conner RD, Dandliker RB, Johnson WL. Mechanical properties of tungsten and steel fiber reinforced Zr41.25Ti13.75Cu12.5Ni10Be22.5 metallic glass matrix composites. Acta Mater 1998;46:6089–102.

[1] For interpretation of color in Fig. 4, the reader is referred to the web version of this article.

[3] Qiao JW, Zhang Y, Chen GL. Fabrication and mechanical characterization of a series of plastic Zr-based bulk metallic glass matrix composites. Mater Des 2009;30:3966–71.
[4] Wang G, Huang YJ, Shen J. Novel TiCuNiCo composites with high fracture strength and plasticity. Mater Des 2012;33:226–30.
[5] Eckert J, Das J, Pauly S, Duhamel C. Mechanical properties of bulk metallic glasses and composites. J Mater Res 2007;22:285–301.
[6] Dandliker RB, Conner RD, Johnson WL. Melt infiltration casting of bulk metallic-glass matrix composites. J Mater Res 1998;13:2896–901.
[7] Kubler A, Eckert J, Schultz L. Nanoparticles in an amorphous Zr55Al10Cu30Ni5 matrix – the formation of composites by mechanical alloying. Nanostruct Mater 1999;12:443–6.
[8] Bian Z, Wang RJ, Wang WH, Zhang T, Inoue A. Carbon-nanotube-reinforced Zr-based bulk metallic glass composites and their properties. Adv Funct Mater 2004;14:55–63.
[9] Hofmann DC, Suh JY, Wiest A, Duan G, Lind ML, Demetriou MD, et al. Designing metallic glass matrix composites with high toughness and tensile ductility. Nature 2008;451:1085–9.
[10] Wu YA, Xiao YH, Chen GL, Liu CT, Lu ZP. Bulk metallic glass composites with transformation-mediated work-hardening and ductility. Adv Mater 2010;22:2770–3.
[11] Zhu Z, Zhang H, Hu Z, Zhang W, Inoue A. Ta-particulate reinforced Zr-based bulk metallic glass matrix composite with tensile plasticity. Scr Mater 2010;62:278–81.
[12] Choi-Yim H, Conner RD, Szuecs F, Johnson WL. Processing, microstructure and properties of ductile metal particulate reinforced Zr57Nb5Al10CU15.4Ni12.6 bulk metallic glass composites. Acta Mater 2002;50:2737–45.
[13] Ferry M, Laws KJ, White C, Miskovic DM, Shamlaye KF, Xu W, et al. Recent developments in ductile bulk metallic glass composites. MRS Commun 2013;3:1–12.
[14] Zhang H, Zhang ZF, Wang ZG, Qiu KQ, Zhang HF, Zang QS. Effects of tungsten fiber on failure mode of Zr-based bulk metallic glassy composite. Metall Mater Trans A – Phys Metall Mater Sci. 2006;37A:2459–69.
[15] Kainer KU. Metal matrix composites. Custom-made materials for automotive and aerospace engineering. Weinheim: WILEY-VCH; 2006.
[16] Chaubey AK, Scudino S, Mukhopadhyay NK, Khoshkhoo MS, Mishra BK, Eckert J. Effect of particle dispersion on the mechanical behavior of Al-based metal matrix composites reinforced with nanocrystalline Al–Ca intermetallics. J Alloys Compd 2012;536. S134-S7.
[17] Ali F, Scudino S, Liu G, Srivastava VC, Mukhopadhyay NK, Khoshkhoo MS, et al. Modeling the strengthening effect of Al–Cu–Fe quasicrystalline particles in Al-based metal matrix composites. J Alloys Compd 2012;536. S130-S3.
[18] Wang H, Li R, Wu Y, Chu XM, Liu XJ, Nieh TG, et al. Plasticity improvement in a bulk metallic glass composed of an open-cell Cu foam as the skeleton. Compos Sci Technol 2013;75:49–54.
[19] Mukherjee S, Schroers J, Zhou Z, Johnson WL, Rhim WK. Viscosity and specific volume of bulk metallic glass-forming alloys and their correlation with glass forming ability. Acta Mater 2004;52:3689–95.
[20] Zheng GP, Shen Y. Simulation of shear banding and crack propagation in bulk metallic glass matrix composites. J Alloys Compd. 2011;509. S136-S40.
[21] Das J, Gtüh A, Klauß HJ, Mickel C, Löser W, Eckert J, et al. Effect of casting conditions on microstructure and mechanical properties of high-strength Zr73.5Nb9CU7Ni1Al9.5 in situ composites. Scr Mater 2003;49:1189–95.
[22] Zhang ZF, He G, Eckert J, Schultz L. Fracture mechanisms in bulk metallic glassy materials. Phys Rev Lett 2003:91.
[23] Zhang QS, Zhang W, Xie GQ, Inoue A. Unusual plasticity of the particulate-reinforced Cu–Zr–based bulk metallic glass composites. Mater Trans 2007;48:2542–4.
[24] Zhang BY, Chen XH, Wang SS, Lin DY, Hui XD. High-strength tungsten wire reinforced Zr-based bulk metallic glass matrix composites prepared by continuous infiltration process. Mater Lett 2013;93:210–4.
[25] Chen G, Cheng JL, Liu CT. Large-sized Zr-based bulk-metallic-glass composite with enhanced tensile properties. Intermetallics 2012;28:25–33.
[26] Eckert J, Das J, Pauly S, Duhamel C. Processing routes, microstructure and mechanical properties of metallic glasses and their composites. Adv Eng Mater 2007;9:443–53.
[27] Chu ZH, Kato H, Wada T, Xie GQ, Yuan GY, Ding WJ. Relationship between the reinforcement size and mechanical properties of Zr-based glassy matrix composites. Mater Trans 2012;53:879–84.
[28] Leonhard A, Xing LQ, Heilmaier M, Gebert A, Eckert J, Schultz L. Effect of crystalline precipitations on the mechanical behavior of bulk glass forming Zr-based alloys. Nanostruct Mater 1998;10:805–17.
[29] Song SX, Bei H, Wadsworth J, Nieh TG. Flow serration in a Zr-based bulk metallic glass in compression at low strain rates. Intermetallics 2008;16:813–8.
[30] Mukai T, Nieh TG, Kawamura Y, Inoue A, Higashi K. Effect of strain rate on compressive behavior of a Pd40Ni40P20 bulk metallic glass. Intermetallics 2002;10:1071–7.
[31] Song KK, Pauly S, Sun BA, Tan J, Stoica M, Kuhn U, et al. Correlation between the microstructures and the deformation mechanisms of CuZr-based bulk metallic glass composites. AIP Adv 2013:3.
[32] Sun BA, Pauly S, Tan J, Stoica M, Wang WH, Kuhn U, et al. Serrated flow and stick-slip deformation dynamics in the presence of shear band interaction in a Zr-based bulk metallic glass. Acta Mater 2013;61. 2281-2281.
[33] Zhang ZF, Zhang H, Pan XF, Das J, Eckert J. Effect of aspect ratio on the compressive deformation and fracture behaviour of Zr-based bulk metallic glass. Philos Mag Lett 2005;85:513–21.
[34] Sarac B, Schroers J. Designing tensile ductility in metallic glasses. Nat Commun 2013:4.
[35] Qu RT, Zhao JX, Stoica M, Eckert J, Zhang ZF. Macroscopic tensile plasticity of bulk metallic glass through designed artificial defects. Mater Sci Eng A – Struct Mater Prop Microstruct Process 2012;534:365–73.
[36] Qu RT, Calin M, Eckert J, Zhang ZF. Metallic glasses: notch-insensitive materials. Scr Mater 2012;66:733–6.